

Amyloid fibrils activate B-1a lymphocytes to ameliorate inflammatory brain disease

Michael Phillip Kurnellas^a, Eliver Eid Bou Ghosn^b, Jill M. Schartner^c, Jeanette Baker^d, Jesse J. Rothbard^a, Robert S. Negrin^d, Leonore A. Herzenberg^b, C. Garrison Fathman^c, Lawrence Steinman^{a,1}, and Jonathan B. Rothbard^{a,c}

^aDepartment of Neurology and Neurological Sciences, Stanford University School of Medicine, Stanford, CA 94305; ^bDepartment of Genetics, Stanford University School of Medicine, Stanford, CA 94305; ^cDivision of Immunology, Department of Medicine, Stanford University School of Medicine, Stanford, CA 94305; and ^dDivision of Blood and Marrow Transplantation, Department of Medicine, Stanford University School of Medicine, Stanford, CA 94305

This contribution is part of the special series of Inaugural Articles by members of the National Academy of Sciences elected in 2015.

Contributed by Lawrence Steinman, October 28, 2015 (sent for review October 5, 2015; reviewed by Jonathan Kipnis and James Rosenbaum)

Amyloid fibrils composed of peptides as short as six amino acids are therapeutic in experimental autoimmune encephalomyelitis (EAE), reducing paralysis and inflammation, while inducing several pathways of immune suppression. Intraperitoneal injection of fibrils selectively activates B-1a lymphocytes and two populations of resident macrophages (MΦs), increasing IL-10 production, and triggering their exodus from the peritoneum. The importance of IL-10-producing B-1a cells in this effective therapy was established in loss-of-function experiments where neither B-cell-deficient (μ MT) nor IL-10^{-/-} mice with EAE responded to the fibrils. In gain-of-function experiments, B-1a cells, adoptively transferred to μ MT mice with EAE, restored their therapeutic efficacy when Amylin 28–33 was administered. Stimulation of adoptively transferred bioluminescent MΦs and B-1a cells by amyloid fibrils resulted in rapid (within 60 min of injection) trafficking of both cell types to draining lymph nodes. Analysis of gene expression indicated that the fibrils activated the CD40/B-cell receptor pathway in B-1a cells and induced a set of immune-suppressive cell-surface proteins, including BTLA, IRF4, and Siglec G. Collectively, these data indicate that the fibrils activate B-1a cells and F4/80⁺ MΦs, resulting in their migration to the lymph nodes, where IL-10 and cell-surface receptors associated with immune-suppression limit antigen presentation and T-cell activation. These mechanisms culminate in reduction of paralytic signs of EAE.

amyloid fibrils | B-1a lymphocytes | experimental autoimmune encephalomyelitis | immune suppression | IL-10

Amyloid fibrils, composed of hexapeptides, when injected into the peritoneum of mice stimulate an immune-suppressive response of sufficient magnitude to reduce the paralytic signs of experimental autoimmune encephalomyelitis (EAE) (1, 2). Analysis of the differential gene-expression pattern in peripheral blood mononuclear cells revealed the amyloidogenic peptides (e.g., Tau 623–628) induced a type 1 interferon (IFN) response. Plasmacytoid dendritic cells were the source of type 1 IFN, which was induced by NETosis arising from neutrophil endocytosis of the amyloid fibrils. Production of the type 1 IFN was therapeutic in Th1-induced adoptive transfer EAE, but exacerbated the paralytic signs of Th17-induced disease, consistent with experiments by Axtell et al. (3). However, not all amyloidogenic peptides induced equivalent amounts of type 1 IFN. The induction of type 1 IFN appeared to correlate with the amount of fibril formation as measured by thioflavin T. A set of peptides with a polar fibril interface (e.g., Amylin 28–33) did not form measurable amounts of fibrils in physiological buffers, induced minimal amounts of type 1 IFN, but nevertheless were therapeutic, reducing IFN- γ , TNF- α , and IL-6 production by peripheral blood mononuclear cells, and thus providing evidence of a second immune-suppressive pathway (2). Further proof of the importance of this second immune-suppressive pathway was the ability of amyloidogenic peptides to be therapeutic in IFN- α / β R^{-/-} animals with EAE (2).

To better define this second immune-suppressive pathway, the induced effects of the amyloid fibrils at the site of injection in the

peritoneum were investigated. The peritoneal cavity contains a variety of specialized cells, including two types of resident macrophages (MΦs), large peritoneal MΦs (LPM) (CD11b^{hi}F4/80^{hi}MHC-II⁺) and small peritoneal MΦs (SPM) (CD11b⁺F4/80^{lo}MHC-II^{hi}), B-1a lymphocytes (CD19^{hi}CD5⁺CD23⁻), and more common components of blood, including the B-2 lymphocytes (CD19⁺CD5⁻CD23⁺), T lymphocytes, mast cells, neutrophils, eosinophils, and NK cells (4). The LPMs (F4/80^{hi}) are more prevalent than the SPMs (MHC-II^{hi}), representing ~90% of peritoneal MΦs. The B-1a and MΦs (LPM+SPM) each comprise ~30% of the total peritoneal cells (4). Several groups have established that B-1a lymphocytes are distinguishable from the more plentiful B-2 lymphocytes and are enriched in body cavities (5). The chemokines and integrins, which are responsible for B-1a localization to the peritoneal cavity and their exodus when activated, have also been defined (6, 7). The B-1a cell population is notable for its constitutive expression of IL-10 (8–10), a well-established immune-suppressive cytokine. IL-10-producing B cells, B10 cells, were shown initially by Janeway and colleagues to be necessary for the recovery from the signs of EAE (11) and were demonstrated subsequently to be immune-suppressive in animal models of multiple sclerosis (12, 13), inflammatory bowel disease (14), collagen-induced arthritis (15), lupus (16), stroke (17), insulin resistance (18), and allergic airway

Significance

IL-10-secreting B lymphocytes and peritoneal macrophages are activated by immunization with amyloid fibrils composed of short peptides resulting in reduction of paralysis and inflammation in mice with experimental autoimmune encephalomyelitis. B-cell-deficient μ MT mice and IL-10 knockout animals were used to establish the critical role of regulatory B cells in the therapeutic mode of action. Reintroduction of B-1a lymphocytes into the μ MT animals reconstituted the ability of the fibrils to ameliorate the paralytic signs, leading to the trafficking of both populations of cells from the peritoneum to secondary lymph organs and not to the CNS. The reduction in CNS inflammation, combined with successful intranasal administration, provides support that this strategy could be translated into an effective human therapeutic.

Author contributions: M.P.K., E.E.B.G., J.M.S., L.S., and J.B.R. designed research; M.P.K., E.E.B.G., J.B., J.J.R., and J.B.R. performed research; M.P.K., E.E.B.G., J.M.S., R.S.N., L.A.H., C.G.F., L.S., and J.B.R. analyzed data; and M.P.K. and J.B.R. wrote the paper.

Reviewers: J.K., University of Virginia; and J.R., Oregon Health Sciences University.

Conflict of interest statement: L.S., J.J.R., and M.P.K. hold patent applications on therapeutic hexapeptides. The applications are licensed to Stanford University. In addition, the sponsor has patent applications on the use of therapeutic hexapeptides. The patents have been licensed to Stanford University.

Data deposition: The data reported in this paper have been deposited in the Gene Expression Omnibus (GEO) database, www.ncbi.nlm.nih.gov/geo (accession no. GSE73026).

¹To whom correspondence should be addressed. Email: steinman@stanford.edu.

This article contains supporting information online at www.pnas.org/lookup/suppl/doi:10.1073/pnas.1521206112/-DCSupplemental.

disease (19). The B10 cells in many of these studies were isolated from the spleen and not the peritoneal cavity, but several authors have argued the similarity of the cell types. Although not identical, the different cells appear to be physiologically similar (20–22).

Maximal immune suppression by B10 cells is observed after the cells are activated through Toll-like receptor (TLR) (12, 23), CD40 (16), or IL-21 ligation (24), all of which induce both an increase in IL-10 production and an egress of the cells from the peritoneum into secondary lymph organs (21, 25). Reduction of symptoms in each of the inflammatory autoimmune diseases correlated with reduction of TNF- α , IL-6, and IFN- γ , a pattern similar to that seen with the administration of the amyloidogenic peptides.

Results

Amyloid Fibrils Are Endocytosed by Peritoneal B Cells and M Φ s.

Amyloid fibrils are endocytosed by M Φ s, dendritic cells, microglia, and neutrophils (26–30). To determine whether peritoneal cells bind the amyloid fibrils, fluorescently labeled Tau 623–628 was mixed with unlabeled peptide at a 1:10 ratio, and the resultant fibrils injected in the peritoneum of healthy, wild-type C57BL/6 mice. After 20 min the peritoneal cells were collected by lavage, stained with anti-CD19 and anti-F4/80, and layered on poly-lysine-coated slides. Confocal microscopy was performed and revealed the presence of intracellular fluorescent fibrils, suggesting that the fibrils were bound and were endocytosed by both B cells (CD19⁺) and M Φ s (F4/80⁺) (Fig. 1 A–C and Movie S1). Viewing multiple fields revealed that the majority of the fluorescent fibrils were bound by F4/80⁺ cells, with a smaller percentage binding CD19⁺ B cells.

Analysis of peritoneal cells isolated from mice injected with the fluorescent amyloid fibrils by flow cytometry confirmed and extended the microscopic study. The composition of the various cell types in the peritoneum can be delineated using 10-color, 12-parameter high-dimensional analysis (Fig. S1 A and B). When the peritoneal M Φ s (both SPM and LPM), mast cells, T, B-2, and B-1 lymphocytes are

delineated with antibodies against CD11b, CD5, and CD19, a more complex pattern of uptake and trafficking is apparent (Fig. 1D). Within 10 min of the FITC-Tau injection more than 70% of the B-1 and B-2 lymphocytes and LPM are FITC⁺. T lymphocytes and mast cells are minimally stained, demonstrating specific binding or uptake by B cells and M Φ s. Five hours after injection of the amyloid fibrils an interesting pattern emerges. The majority of the CD11b^{hi} population is significantly reduced from ~45–3% of total peritoneal cells (Fig. S1C). Most of the B-1a population has disappeared, with the remaining cells being FITC-Tau⁻ (Fig. S1D). The majority of T lymphocytes and mast cells remained unstained with the fibrils. Collectively, the flow cytometry studies revealed that B cells and M Φ s bind the fibrils, and that the relative number of B-1a lymphocytes (CD19^{hi}CD5⁺) and the LPMs (CD11b^{hi}) was dramatically reduced 5 h after injection of the amyloid.

We asked if fibrils were selectively toxic to the B-1a and LPMs. This theory was ruled unlikely when no cell death was observed when the peritoneal cells were cultured in vitro with the fluorescent amyloid (Fig. S2). Rather than killing the cells, a testable hypothesis was that the fibrils induced the exodus of the two cell populations from the peritoneum.

μ MT and IL-10 Knockout Mice Do Not Respond to Therapy. To determine the importance of B lymphocytes in the mode of action of the amyloid fibrils, EAE was induced in μ MT mice, which because of a mutation in the transmembrane region of IgM lack expression of all subtypes of B cells (31). The paralytic signs of the disease were induced in these animals, consistent with induction of the disease by T lymphocytes, but neither Tau 623–628, nor Amylin 28–33 was therapeutic compared with the effect seen in wild-type mice (Fig. 2 A–C). The therapeutic activity of the amyloidogenic peptides appeared to require the presence of B cells, most likely B-1a cells based on the composition of the peritoneum and the microscopy.

B-1a cells are characterized by the constitutive expression of relatively large amounts of IL-10 (9, 10). To establish whether

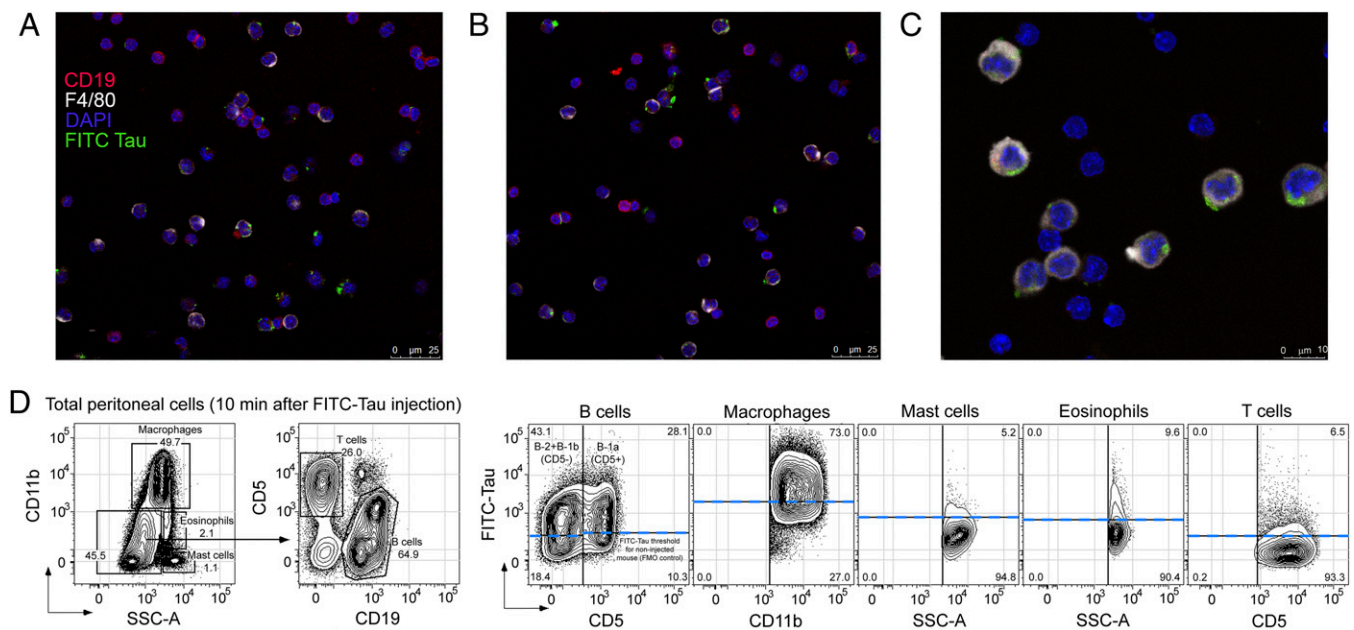


Fig. 1. Amyloid fibrils composed of Tau 623–628 bind and are endocytosed by B-1a lymphocytes (CD19^{hi}CD5⁺) and LPMs (CD11b^{hi}F4/80^{hi} peritoneal M Φ s). (A and B) A composite of a confocal image (40 \times magnification) and (C) a single z-cut (63 \times) from a movie constructed from the set of confocal images (Movie S1) of peritoneal cavity cells from wild-type mice injected with 10 μ g FITC-Tau 623–628 and stained with rat anti-mouse CD19 (PE), F4/80 (Alexa Fluor 647), and DAPI. Cells were visualized using a Leica TCS SP8 white light laser confocal microscope. (D) Wild-type mice were injected with 10 μ g FITC-Tau 623–628 and peritoneal cells were isolated after 10 min and compared with peritoneal cells from an uninjected animal. The cells were washed and stained with rat anti-mouse CD11b (PE), CD19 (Pacific blue), CD5 (APC), CD3 (PerCP-Cy5.5), and propidium iodide (PI) for viability. The gates demarcating the different cell types are shown in the two left panels (10 min postinjection), and the amount of staining with FITC-Tau for each cell type is shown in the five right panels.

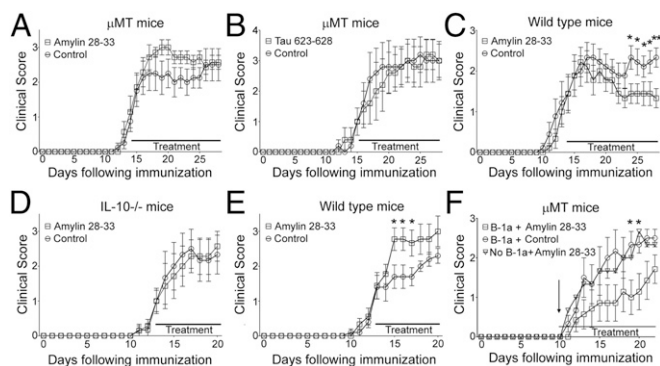


Fig. 2. B-1a cells and IL-10 are necessary for therapeutic efficacy of amyloidogenic peptides. μ MT mice were treated daily with intraperitoneal injections of 10 μ g (A) Amylin 28–33 (*n* = 10) or (B) Tau 623–628 (*n* = 10) at onset of symptoms. (C) Wild-type EAE mice were treated daily intraperitoneally with 10 μ g Amylin 28–33 (*n* = 10). (D) IL-10-deficient (*n* = 7) and (E) wild-type (*n* = 10) mice were treated daily with 10 μ g Amylin 28–33. Values in graph represent mean \pm SEM; **P* < 0.05 and ***P* < 0.005 by Mann–Whitney *U* test. (F) Adoptive transfer of 3.5×10^5 B-1a cells into μ MT mice before the signs of EAE were treated daily intraperitoneally with 10 μ g Amylin 28–33 or control buffer (*n* = 6). Mice without transfer of cells were treated with 10 μ g Amylin 28–33. Values in graph represent mean \pm SEM; **P* < 0.05 by Mann–Whitney *U* test. All experiments were repeated at least twice.

this cytokine was central to therapeutic effects of the peptides and to correlate the activity with this B-cell subtype, 10 μ g Amylin 28–33 was used to treat EAE induced in IL-10 knockout animals (Fig. 2D and E). Again, the peptide was ineffective in this animal model, establishing that both IL-10 and B lymphocytes are central to the therapeutic activity of the amyloidogenic peptides.

Adoptive Transfer of B-1a Cells Restored Therapeutic Efficacy of Amyloidogenic Peptides in μ MT Animals. The characteristics of peritoneal B-1a cells clearly correlate with the apparent requirements for therapeutic function. Thus, replacement of this population in μ MT mice should restore the immunosuppressive activity of the amyloid fibrils. Peritoneal cells were isolated from C57BL/6 mice, and B-1a cells (CD19^{hi}CD5⁺) were purified by cell sorting. EAE was induced in μ MT mice and, on day 10 after induction, before the appearance of clinical signs, the mice were injected in the peritoneal cavity with purified B-1a cells (3.5×10^5 cells). The mice were divided into two groups and treated daily with Amylin 28–33 (10 μ g) or buffer alone (Fig. 2F). μ MT mice induced with EAE that did not receive B-1a cells but were treated with Amylin 28–33 were used for comparison. Interestingly, only mice that received the transfer of B-1a cells treated daily with the amyloidogenic peptide exhibited reduced paralytic signs of EAE. Adoptive transfer of untreated B-1a cells was as ineffective as buffer control, establishing not only the importance of B-1a cells but that the cell population needs to be activated by the fibrils to be effective. This finding corroborates studies that regulatory B cells are more potent suppressors of autoimmunity than their nonactivated counterparts (24, 32).

Amyloidogenic Peptides Induce Exodus of B-1a Cells and LPM from the Peritoneal Cavity. Real-time measurement of bioluminescence demonstrated that the amyloidogenic peptides induce an exodus of both B-1a cells and LPM from the peritoneum. B-1a cells (CD19^{hi}CD5⁺CD23⁻) and LPMs (CD11b^{hi}F4/80^{hi}) were sorted from peritoneal cells isolated from luciferase transgenic mice, C57BL/6 L2G85 (H-2^d) [B6.FVB-*Ptprca* Tg(CAG-luc,-GFP)L2G85Chco *Thy1a*/J], which express the CAT-luc-eGFP, L2G85 transgene. In the initial experiment 1×10^5 and 2×10^5 B-1a cells were injected into the peritoneum of C57BL/6 female albino mice, followed by injection of 10 μ g of Tau 623–628 to activate the

lymphocytes, and 300 μ g/g body weight of the substrate luciferin, to initiate the enzyme-substrate reaction for the bioluminescence imaging. The location of the luciferase-expressing cells was monitored by imaging the mice every 5 min for 75 min (Fig. 3A and Fig. S3). The diffuse distribution of the luminescence, corresponding to the peritoneal cavity, seen at early times, was reduced in intensity over time, with focal regions of intensity appearing to localize in inguinal lymph nodes beginning at 35 min (Fig. 3A). Measuring the total number of photons per second in the abdominal region revealed a rapid, dose-dependent, reduction of light emitted over the 75 min of the experiment (Fig. 3B). Even though the size of the signal was proportional to the number of cells injected, the rate of reduction or slope of the curve was equivalent in the two animals. Such a result is consistent with the amyloid fibrils triggering egress of the B-1a cells from the peritoneum.

The experimental design of the initial experiment did not allow the reduction of the signal to be assigned unequivocally to the migration of the lymphocytes because the concentration of the luciferin also diminishes during the 75 min of examination. To better assign the basis of the reduction of luminescence to the migration of the luc⁺ cells, a second experiment was performed with four recipient mice. Two were injected with 1×10^6 luc⁺ M Φ s (LPMs), a third with 2×10^5 B-1a cells, and fourth mouse serving as a control was injected only with luciferin. In this experiment, the mice were subsequently injected with 10 μ g of Tau 623–628 and luciferin. Bioluminescence was measured immediately after the injection of luciferin and 5 min later. After 30 min the mice were re-injected with luciferin and the resultant luminescence measured. A similar injection and measurement was done after 60 min. The multiple injections of luciferin kept the drug level close to saturation during all measurements, so that any changes were caused by migration and trafficking. Using 1×10^6 LPMs produced a vivid signal at all time points, the details of which were similar to that observed in the initial experiment, increased distribution of light with time, along with a concentration in an area over inguinal lymph nodes (Fig. 3C). In the mouse receiving the B-1a cells, a less-intense signal was observed, but nevertheless evidence of exodus of the luc⁺ cells from the peritoneum was apparent (Fig. S4). When photons per second over the full body of each mouse were measured and plotted versus

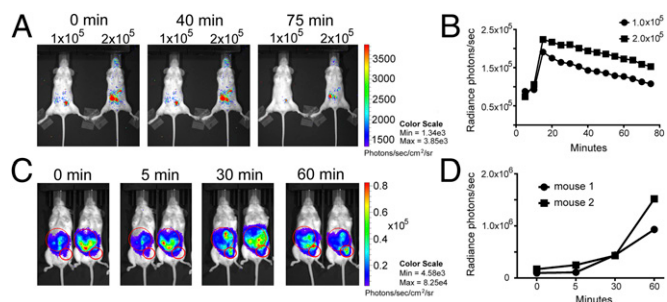


Fig. 3. Real-time measurement of trafficking of adoptively transferred B-1a lymphocytes and LPMs using bioluminescence induced by amyloidogenic peptides. (A) 1×10^5 and 2×10^5 B-1a sorted cells were injected intraperitoneally with the substrate luciferin into C57BL/6 albino mice and bioluminescence images were obtained using a CCD camera serially every 5 min. Bioluminescent signal was detectable from the peritoneal area, diminishing with time, and relocalizing in the inguinal lymph node area. (B) Quantification of B-1a luc⁺ cell distribution by measuring light emission from the C57BL/6 albino mice over time after injection of Tau 623–628. (C) 1×10^6 luc⁺ LPMs were injected intraperitoneally into C57BL/6 albino mice and luciferase was re-injected every 30 min before an image was obtained. The M Φ s egressed from the peritoneum (larger circle) and migrated to different tissues including the inguinal lymph nodes (smaller circle). (D) Quantification of M Φ s cells migrating to the lymph nodes from the peritoneum by measuring the light emission. BLI measured from the lymph nodes increased by 10-fold at 60 min compared with the initial measurement at 5 min.

time, there was a proportional increase in signal as a function of time. In the case of the area corresponding to the inguinal lymph nodes, there was close to a 10-fold increase in luminescence from the measurement at 5–60 min (Fig. 3D). Collectively, the imaging experiments establish that the amyloidogenic peptides induce a migration of both B-1a cells and LPMs from the peritoneum to the inguinal lymph nodes.

To further examine how amyloid fibrils induce an exodus of B-1a cells and LPMs, a series of experiments was performed using IL-10 reporter mice in which IL-10 and GFP are connected via an internal ribosome entry site (IRES) to create a bicistronic message marking IL-10-secreting cells with fluorescence (33). Because LPS is known to induce B-1a cell migration from the peritoneum to the spleen, the effects of the amyloid fibrils were compared with those effects observed with the TLR4 ligand (34, 35). To allow for maximal changes in IL-10 transcription, and because the resulting GFP is relatively long-lived, the experiment was designed to confirm exodus, and to identify possible sites of migration. Because previous experiments established that ~80% of the B-1a and LPMs exited the peritoneum at 5 h, time points for analysis were chosen at 30 min and at 24 h after injection of the fibrils. Three groups of three IL-10 reporter C57BL/6 female mice were injected with 10 μg LPS, 10 μg Amylin 28–33, or buffer alone, and after 5 or 24 h the peritoneal cells were lavaged, the spleen and inguinal and axillary lymph nodes were dissected with the lymph nodes being pooled, and single cell suspensions were prepared and delineated using 10-color, 12-parameter high-dimensional analysis (Fig. S5 A and B). Similar cells and tissues also were taken from three wild-type mice as additional controls. Injection of LPS not only increased the relative numbers of IL-10-secreting B-1a cells (from ~25% to ~40% in 24 h), but it also induced higher levels of IL-10, as evidenced by higher levels of GFP median fluorescence intensity.

In contrast, injection of Amylin 28–33 did not increase IL-10 secretion; however, there was a decrease in the number of IL-10⁺ B-1a cells and LPMs in the peritoneum after 24 h that was not observed with LPS (Fig. 4 and Fig. S5C).

In the spleen, LPS induced an increase in both the number of B-1a cells and the amount of IL-10 expressed per cell 24 h after injection (Fig. 4). Amylin fibrils did not induce an increase of the B-1a cells in spleen, but rather an apparent reduction in both numbers and IL-10 expression. The opposite pattern was observed in the pooled lymph nodes. LPS resulted in a slight increase of B-1a cells in the pooled lymph nodes. Injection of Amylin 28–33 increased the percentage of B-1a cells in the lymph node, with an increase in the amount of IL-10 expression. In IL-10 reporter mice with EAE, an additional pattern was observed. No significant increase in B-1a cells were detected in the brain or spinal cord (Fig. S6), consistent with the hypothesis that the B-1a and MΦ populations migrate to the secondary lymph organs, and not to the primary sites of inflammation.

The experiments using the IL-10 reporter mice revealed that both LPS and the fibrils activated B-1a cells, SPM, and LPM, inducing IL-10 gene expression and subsequent exodus from the peritoneum. However, the magnitude of the increase and the details of the directions of migration differ. As previously reported, LPS activates the B-1a cells, resulting in greater production of IL-10 and migration to the spleen (25), whereas the fibrils predominantly induced migration to the lymph nodes. Interestingly only B-1a cells expressing CD80/86 secrete IL-10, and IL-10-secreting B-1a cells were found in lymph nodes of normal animals with the relative number increased with injection of amylin fibrils. The flow cytometry experiments establish that the amyloidogenic peptides activate both B-1a cells and LPMs, resulting in both cell types trafficking to the draining lymph nodes.

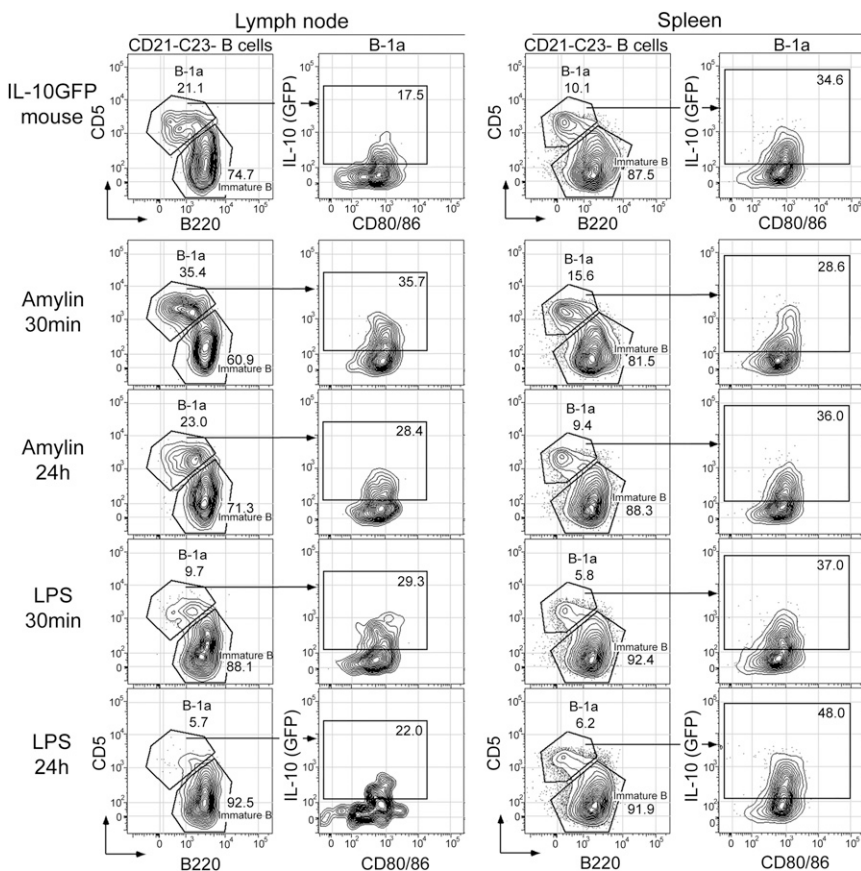


Fig. 4. Effects of injection of Amylin 28–33 compared with LPS on the migration of IL-10-producing cells to the spleen and lymph nodes in IL-10 reporter mice. Lymph nodes (Left) and spleen (Right) were harvested from IL-10 reporter mice 30 min and 24 h after intraperitoneal injection of either 10 μg Amylin 28–33 or 10 μg LPS. The panels shown in the first row represent the percentage of B-1a cells in uninjected mice. The percentage of B-1a cells in both lymph nodes and spleen was increased 30 min after Amylin injection. In contrast, LPS reduced the percentage of B-1a cells, especially 24-h postinjection. B-1a cells, in both lymph nodes and spleen, represent the major source of IL-10 (i.e., GFP⁺). In contrast, follicular B-2 cells did not produce any detectable levels of IL-10 in all conditions analyzed here, including in uninjected mice. Tissues were processed into single-cell suspension and stained with an 11-color stain set panel using rat anti-mouse CD11b (Pacific blue), CD80/CD86 (biotin-Qdot605-streptavidin), CD21 (APC), IgM (Alexa Fluor 700), B220 (APC-Cy7), CD23 (PE), CD5 (PE-Cy5), CD19 (PE-Cy5.5), Gr-1 (PE-Cy7), and PI (viability). Total B cells (CD19⁺) were identified as shown in Fig. S5. CD21⁺CD23⁺ B cells were further analyzed for their surface expression of CD5 and B220 to identify B-1a (CD5⁺B220^{lo}) and immature B (CD5⁺B220^{hi}) cells.

Differential Gene Expression in B-1a Lymphocytes and MΦs Induced by Amyloid Fibrils. The migration of B-1a cells and LPMs after the injection of amyloid fibrils was consistent with the activation of both cell types. However, the receptors for the fibrils has not been defined for either the B-1a cells or the peritoneal MΦs. Unlike migration induced by LPS stimulation, the fibrils composed of the peptides do not bind to TLR2 or MD2/TLR4. A set of over 15 different amyloidogenic peptides was screened for binding to commercially available HEK cells transfected with murine TLR2 or MD2/CD14/TLR4. The transfected cells contained a secretable form of alkaline phosphatase under the control of an NF-κB promoter. None of the amyloid fibrils composed of the varying peptides was positive in this assay (Fig. S7).

To confirm and increase the understanding of how the fibrils are activating the peritoneal cells, differential gene induction in purified B-1a and LPMs was analyzed. Making such measurements was complicated by the fact that LPS and the fibrils induce a rapid migration of the relevant cells from the peritoneal cavity, and consequently a high percentage would not be isolated by lavage an hour after injection. To minimize the population bias, and yet allow sufficient time for the fibrils to induce gene expression, cells were isolated between 30 and 40 min after injection of LPS or the amyloidogenic peptides. Consequently, the analysis is limited to gene expression in the 30–40 min after stimulation. Peritoneal cells from groups of three C57BL/6 female mice were isolated after injection with either LPS, fibrils composed of Amylin 28–33 or Tau

623–628, or buffer control. B-1a cells (CD19^{hi}CD5⁺CD23⁻) and LPMs (CD11b^{hi} MΦs) from the four groups of three mice were sorted into TRIzol, RNA extracted, and gene expression measured using a murine Agilent whole-genome expression microchip. Differential gene expression of the B-1a and LPMs was calculated by subtracting the gene expression data from cells isolated from mice injected with buffer from expression data from mice injected with LPS or the amyloid fibrils (Fig. 5A). All microarray data are available at the Gene Expression Omnibus (GEO) database (GEO series accession no. GSE73026).

The pattern of gene expression induced by LPS is well characterized in both cell types binding to CD14/TLR4 (36, 37), resulting in the induction of a wide spectrum of proinflammatory mediators, such as *IL-6*, *TNF-α*, *type 1 IFN*, *Serpins*, *IL-1α* and *-β*, chemokines *CXCL10*, *CXCL3*, *MYD88*, and over 50 genes known to be induced by RelA/p65 NF-κB (38). In peritoneal MΦs amyloidogenic peptides stimulated a distinctly different set of genes from those induced by LPS. To portray the variation, a heatmap of the correlation of a set of 730 annotated genes induced by LPS in MΦs demonstrates the gene-expression signature induced by the two amyloidogenic peptides is similar and distinct from the pattern generated by injection with LPS (Fig. 5A). The majority of genes preferentially induced by the fibrils corresponded to MΦ stimulation, cytokine production, oxidative phosphorylation, and mitochondrial dysfunction pathways. The oxidative phosphorylation pathways were induced, demonstrated by the expression of a large

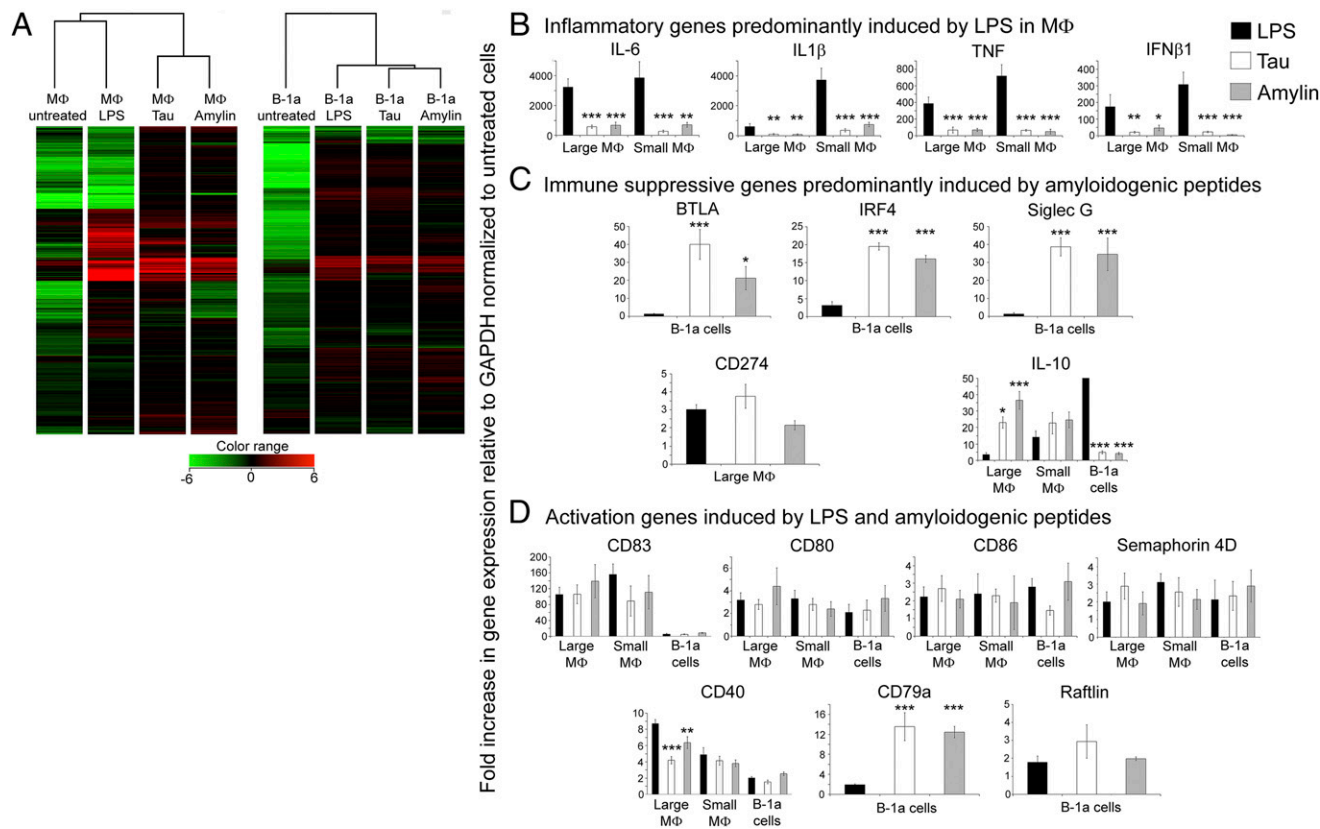


Fig. 5. Amyloid fibrils, composed of either Tau 623–628 or Amylin 28–33, induce a different pattern of gene expression than LPS in B-1a lymphocytes and peritoneal MΦs, SPM, and LPM. (A) Differential gene expression (720 annotated genes) expressed as a heatmap induced by LPS and the two types of amyloid fibrils. RNA isolated from purified B-1a lymphocytes and CD11b^{high} MΦs isolated from groups of three C57BL/6 mice injected with either 10 μg LPS, Amylin 28–33, Tau 623–628, or buffer. Each of the RNA samples was hybridized to a microarray plate (SurePrint G3 Mouse; Agilent Technologies) and quantified and analyzed using GeneSpring and Ingenuity software. Measurement by qPCR of gene induction compared with cells from uninjected animals of sets of genes representing (B) inflammatory cytokines, (C) immune suppressive genes, or (D) activation genes. Values in the graphs represent mean ± SEM; **P* < 0.05, ***P* < 0.005, and ****P* < 0.0005 by one-way ANOVA with Dunnett’s Multicomparison test. Graphs represent the results of three separate measurements. The full set of data has been deposited in the GEO databank.

number of mitochondrial genes composing the five complexes involved in mitochondrial electron transport and ATP production, characteristic of amyloid fibril interactions with mitochondria (39).

In the case of B-1a cells, a less-vivid difference between LPS and the peptides is seen, but the patterns induced by the two types of fibrils are distinguishable from that of LPS. In contrast, with MΦs, LPS and the amyloidogenic peptides both induced a pattern of expression characteristic of B-cell activation. The amyloidogenic peptides stimulated expression of a set of proteins involved in signalosome formation (raftlin, CDC42, CDC42 small effector protein), calcium release (stim-1, orai-1 and -3), BcR (CD79, Syk, Lyn, PI3K, Akt, m-Tor, Bcl2A1d, c-src, PTEN, and Vav-1), and CD40 signaling (Traf-2, -4, and -5), all of which are known to induce NF-κB activation. Even though the LPS and amyloidogenic peptides induced a large number of similar genes involved in lymphocyte activation, a clear distinction could be observed, with the amyloidogenic peptides inducing a set of immunosuppressive proteins, such as B- and T-lymphocyte attenuator (BTLA), interferon regulatory factor 4 (IRF4), and Siglec G.

To confirm the gene-expression data from the chip, a set of genes was analyzed by quantitative PCR (qPCR) (Fig. 5 B–D). In these experiments RNA was isolated from B-1a, large and small MΦs using identical methods and similar times after injection of the stimulants, as was done for the microarray. Consistent with the pathway analysis of the chip data, *IL-6*, *TNF*, *IL-1β*, and *IFN-β1* were significantly induced by LPS in the peritoneal MΦs, and minimally by the peptide fibrils. Interestingly, the SPMs (CD11b⁺F4/80^{lo/-} MΦs) uniformly expressed a greater amount of the inflammatory genes, particularly *IL-1β*, than the LPMs (CD11b^{hi}F4/80^{hi} MΦs). In the peritoneum, SPMs compose less than 10% of the MΦ population, are not the dominant cell type that endocytose the fibrils, nor do they represent the major depleted population of cells after injection of LPS or the fibrils. In contrast, the fibrils induced a set of genes associated with immune regulation, *BTLA*, *Siglec G*, and *IRF4* in B-1a cells, and *CD274* in LPMs. LPS induced some, but not all of these genes. The third set of genes analyzed were those known to be associated with cell activation. *CD40*, *CD80*, *CD86*, and *semaphorin 4D* were induced by both LPS and the fibrils in B-1a cells and both types of MΦs. *CD83* was induced by both stimuli principally on the MΦs, whereas *CD79a* and *Raftlin* were induced on the B-1a cells.

The pattern of gene expression indicated that both types of amyloid fibrils activated the B-1a cells and both populations of the peritoneal MΦs (SPM and LPM). *IL-10* gene expression was increased in both B-1a and LPMs, two of the cell types shown to traffic to lymph nodes. The induction of *BTLA* and *Siglec G* in the B-1a cells would increase their immune regulatory phenotype. The expression of *IL-10* in the LPMs is consistent with the conversion of these cells to a M2 phenotype, also believed to suppress inflammatory responses.

Nasal Delivery Retains the Therapeutic Efficacy of the Amyloidogenic Peptides. Peritoneal injection is not a practical route of drug administration for activation of B-1a cells in humans. However, B-1a cells also are plentiful in the pleural cavity of both mice and humans (40). To examine whether this alternative route of administration is both practical and sufficient for treatment, 10 μg Amylin 28–33 was administered daily intranasally to groups of 10 C57BL/6 mice with EAE. The paralytic signs of the disease were reduced in a fashion equivalent to that seen when the amyloidogenic peptide is injected intraperitoneally (Fig. 6A). In addition, splenocytes from peptide-treated mice exhibited a reduction in secretion of proinflammatory cytokines, IL-6, IFN-γ, IL-2, and IL-17, in response to myelin oligodendrocyte glycoprotein_{35–55} (MOG_{35–55}) challenge in vitro, compared with control (Fig. 6B), a pattern identical to when Amylin 28–33 was injected (1).

The success of the intranasal delivery is consistent with a mode of action in which the B-1a cells play a central role, but also

establish a potential route of administration that can be used in clinical trials in human patients.

Discussion

Amyloid fibrils composed of amyloidogenic peptides exhibit a wide spectrum of biological activities, the sum of which results in an immune-suppressive response of sufficient magnitude to be therapeutic in a robust model of multiple sclerosis. As molecular chaperones, they bind a spectrum of proinflammatory mediators in plasma (1). In blood they are endocytosed by neutrophils, which induce the production of nets, which in turn induces plasmacytoid dendritic cells to secrete type 1 IFN (2). In this paper, a third mode of action is defined wherein the fibrils bind and activate both B-1a lymphocytes and a subset of peritoneal MΦs known as LPMs (4), which are induced to increase *IL-10* transcription and migrate out of the peritoneum to secondary lymph organs. The exodus results in the selective delivery of *IL-10* to immunological sites shared with inflammatory T lymphocytes and their complementary antigen-presenting cells. *IL-10* is known to effectively inhibit both inflammatory cell populations, with reduction of the production of proinflammatory cytokines, *IL-6*, *TNF-α*, and *IFN-γ* (41). This reduction of cytokines was the hallmark of the immune suppression induced in EAE by the amyloidogenic peptides (2). The peritoneal cells do not appear to migrate to the sites of inflammation in the CNS, and consequently do not need to cross the blood–brain barrier.

Knockout mice were central to establishing the mechanism. The inability of the peptide amyloid to reduce inflammation in B-cell-deficient μMT mice with EAE highlighted the importance of B cells. Flow cytometry and fluorescent microscopy were used to establish that in the peritoneum the relevant target in the B-cell population was B-1a lymphocytes, a known secretor of *IL-10* (9, 10). Additional support for the role of *IL-10*-secreting B-1a cells was the failure of *IL-10*^{-/-} mice with EAE to respond to the amyloid therapy. Further support for the role of *IL-10*-secreting B-1a cells in the mechanism of action came from classic adoptive-transfer experiments. The adoptive transfer of purified B-1a cells into μMT mice converted the B-cell-deficient mice from nonresponders to responders to the amyloidogenic peptides. An important point was that the transfer of the B-1a cells alone did not reduce the paralytic signs of EAE. The signs were reduced only after injection of the fibrils, which were shown to activate the transferred population.

Once activated, both the B-1a lymphocytes and the LPMs leave the peritoneum, but their trafficking patterns are less clear. Previous studies established that LPS activation of B-1a cells resulted in trafficking from the peritoneum to the spleen (35). Tedder and colleagues have shown activation of a splenic population of

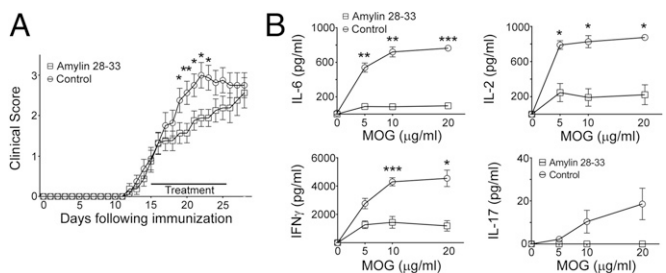


Fig. 6. Intranasal delivery of Amylin 28–33 reduces the clinical signs of EAE. (A) Mice with EAE were treated daily intranasally with 10 μg Amylin 28–33 ($n = 16$) for 10 d at onset of symptoms. Values in graph represent mean \pm SEM; $*P < 0.05$ and $**P < 0.005$ by Mann–Whitney U test. Experiments were repeated twice. (B) Splenocytes from EAE mice treated with 10 μg Amylin 28–33 were stimulated with 0, 5, 10, and 20 μg/ml MOG_{35–55} and the levels of cytokines IL-6, IFN-γ, IL-2, and IL-17 were measured ($n = 3$). Values in graph represent mean \pm SEM; $*P < 0.01$, $**P < 0.001$, and $***P < 0.0001$ by Student's t test.

regulatory B cells that migrate to draining lymph nodes (19, 24, 42). Using real-time measurement of the trafficking of adoptively transferred luminescent B-1a cells and LPMs revealed that activation with the amyloid fibrils resulted in migration to inguinal lymph nodes. Flow cytometric studies using IL-10 reporter mice supported both the timing and the location of the trafficking. The receptors for the fibrils has not been defined for either the B-1a cells or the peritoneal MΦs. However, the fibrils composed of the peptides do not bind to TLR2 or CD14/MD2/TLR4 expressed in HEK cells (Fig. S7).

In the case of an intraperitoneal injection, the activation of the peritoneal cells would be expected to precede any biological activity stimulated by the fibrils in serum, and consequently should contribute to a greater percentage of the response. The proposed mode of action is consistent with the relatively long pharmacokinetics and pharmacodynamics of the amyloidogenic peptides. The fibrils themselves will have an expected half-life measured in minutes. However, the fibrils activate a set of peritoneal cells, which are the therapeutic agents and migrate to the secondary lymph organs, where they secrete immune-suppressive IL-10. The cells do not appear to traffic to the sites of inflammation in the spine and the brain in mice with EAE and do not cross the blood–brain barrier, which is consistent with the documented scarcity of B lymphocytes in EAE lesions (43). The fate of the activated B-1a lymphocytes and the LPMs reflects the pharmacodynamics of the therapy, and not the fate of the amyloidogenic peptides. Similarly in the pharmacokinetics of the response, the 1- or 2-d delay in the reduction of the paralytic signs after the injection of the fibrils reflects the time necessary for the activation and migration of the peritoneal cells, combined with the immune suppression of a sufficiently large percentage of the inflammatory T lymphocytes. Reciprocally, cessation of therapy results in a 24- to 72-h delay in the return of the paralytic signs, which is consistent with the half-life of the immune suppression induced by the IL-10-producing cells, and not the half-life of the fibrils. In many respects the therapeutic effects of the fibrils resemble pharmacokinetics of adoptive cell therapy rather than a classic small-molecule therapeutic. The proposed mechanism of the migration of the immune-suppressive cells to secondary lymph organs, where they suppress both circulating inflammatory antigen-presenting cells and T lymphocytes, is consistent with published studies on B-regulatory cells (21, 44). The mechanism also argues that this therapeutic approach might be beneficial in a number of systemic inflammatory indications.

The fibrils induce a concomitant inflammatory response, most evidently in the SPMs, with induction of IL-1 β , TNF- α , and IL-6. Why this response does not dominate the immune-suppressive effects can best be explained by the large excess of LPMs and B-1a lymphocytes and their greater propensity to rapidly traffic out of the peritoneum to the secondary lymphoid tissues.

The effective therapy with the nasal administration of the fibrils bodes well for translation to human therapy. The known predominance of B-1a lymphocytes in the pleural cavity predicts that such a route might be successful, and that peptides can be readily administered as powders, making inhalation a practical alternative to an injection.

To our knowledge, the amyloidogenic peptides are the first therapeutic that targets regulatory B cells. The extensive list of indications in which this population of cells limits inflammation is supportive of the potential for the strategy of using the amyloid fibrils in a spectrum of inflammatory diseases.

Methods

Induction of Active EAE in Mice by Immunization with MOG and Adjuvant. EAE was induced in female wild-type C57BL/6 mice or μ MT and IL-10-deficient mice on C57BL/6 background (Jackson Laboratories) by procedures previously described. Briefly, EAE was induced at 9 wk of age by subcutaneous immunization in the flank with an emulsion containing 200 μ g MOG_{35–55} (MEVGWYRSPFSRVVHLYRNGK) in saline and an equal volume of complete Freund's adjuvant containing

4 μ g/mL *Mycobacterium tuberculosis* H37RA (Disco Laboratories). All mice were given 400 ng of pertussis toxin (List Biological) intraperitoneally at 0- and 48-h postimmunization. The signs of neurological impairment were scored as follows: 0, no clinical disease; 1, tail weakness; 2, hindlimb weakness; 3, complete hindlimb paralysis; 4, hindlimb paralysis and some forelimb weakness; 5, moribund or dead. When animals exhibited an average of level one to two for clinical signs they were injected in the peritoneum with 10 μ g of Tau 623–628, Amylin 28–33 peptide, or PBS daily. For intranasal inoculation, 10 μ g of Amylin 28–33 in 10 μ L PBS was gradually released into the nostrils of anesthetized mice. All animal protocols were approved by the Institutional Animal Care and Use Committee at Stanford University.

Adoptive Transfer of B-1a Lymphocytes. B-1a lymphocytes were purified by cell sorting of peritoneal cells from wild-type C57BL/6 mice. Ten days following induction of active EAE in μ MT mice, 3.5×10^5 B-1a cells were transferred into the peritoneal cavity. Mice were treated with 10 μ g Amylin 28–33 or PBS daily for 14 d. Control μ MT mice with EAE were treated with 10 μ g Amylin 28–33 without transfer of B-1a lymphocytes. Mice were examined daily for clinical signs of EAE and were scored on a five-point scale described above.

Microscopy. C57BL/6 female mice were injected with FITC-Tau 623–628, and peritoneal cells were isolated after 10 min, washed, stained with rat anti-mouse CD19 (PE), F4/80 (Alexa Fluor 647), and DAPI, washed, and plated on poly-lysine-coated microscope slides. Cells were visualized using a Leica TCS SP8 white light laser confocal microscope.

Bioluminescence Experiments. B-1a lymphocytes and peritoneal MΦs were purified by cell sorting of peritoneal cells isolated from luciferase transgenic mice [B6.FVB-*Ptprca* Tg(CAG-luc, GFP)L2G85Chco *Thy1a*/J], which express the CAT-luc-eGFP, L2G85 transgene. In the initial experiment 2×10^5 and 1×10^5 B-1a cells were injected in the peritoneum of C57BL/6 female albino mice [B6(Cg)-Tyr^{c-2j}/J], followed by injection of 10 μ g of Tau 623–628 to activate the lymphocytes, and 0.3 mg/g body weight of luciferin substrate (β -luciferin firefly L-8220 Biosynth) to initiate the bioluminescence imaging. The location of the luciferase-expressing cells was measured by imaging every 5 min for 75 min.

To confirm the diminution of luminescence was a result of the trafficking of the luc⁺ cells, and not the degradation of the luciferin, two C57BL/6 albino mice were injected with 10^6 luc⁺ peritoneal MΦs, a third with 2×10^5 B-1a cells, and a fourth mouse serving as a BLI control was injected with luciferin only. The mice were subsequently injected with 10 μ g of Tau 623–628 and 0.3 mg/g of luciferin. Bioluminescence was measured immediately after the injection of luciferin and 5 min later. After 30 min the mice were re-injected with luciferin and the resultant luminescence measured. A similar injection and measurement was done after 60 min. The multiple injections of luciferin kept the drug level close to saturation during all measurements, so that any changes were because of cell movement. Mice were imaged using an IVIS100 charge-coupled device (CCD) imaging system (Xenogen). Imaging data were analyzed and quantified with Living Image software 4.4 (Xenogen).

Peptide Synthesis and Preparation of FITC-Tau. Peptides were synthesized using solid-phase techniques and commercially available Fmoc amino acids, resins, and reagents (PE Biosystems and Bache) on an Applied Biosystems 433A peptide synthesizer, as previously described (45). Purity of the peptides was shown to be greater than 90% using a PE Biosystems 700E HPLC and a reverse-phase column (Alltech Altima). The molecular weight of the peptides was confirmed using matrix-assisted laser desorption mass spectrometry.

To prevent excess amounts of fluorophore in the fibrils, Tau 623–628 was mixed at a ratio of 10:1 with an analog with FITC attached to the amino terminus of Tau 623–628 with an amino caproic acid linker. The resulting fibril mixture is referred to in the text as FITC-Tau.

RNA Isolation, Chip Hybridization, and qPCR. Total RNA was extracted from FACS-purified B-1a lymphocytes and peritoneal MΦs pooled from three to six C57BL/6 female mice injected with 10 μ g of LPS, Tau 623–628, Amylin 28–33, or PBS using TRIzol reagent and the Qiagen RNeasy micro kit. First-strand cDNA was synthesized with 30–50 ng of total RNA using SuperScript III first-strand synthesis supermix for qRT-PCR. qPCR assays were performed using the 7900HT Fast Real Time PCR System (Applied Biosystems), and the Taqman Gene Expression Arrays (Applied Biosystems) using commercially available primers (ABI). All assays were performed according to the manufacturer's instructions. The comparative Ct method for relative quantification ($\Delta\Delta$ Ct) was used to compare gene expression. Housekeeping-gene expression was used to normalize expression using the following equation: normalized expression = $2^{-(Ct_{\text{house-keeping gene}} - Ct_{\text{gene}})}$.

Gene-expression changes associated with treatment with LPS, Amylin 28–33, and Tau 623–628, were quantified using a microarray (SurePrint G3 Mouse; Agilent Technologies). RNA quality was shown to be suitable for microarray experiments (2100 Bioanalyzer, Agilent Technologies). Analysis and quantitation of the data were done using GeneSpring and Ingenuity software.

Flow Cytometry. Peritoneal cavity cells were obtained by flushing the peritoneal cavity with 10 mL of cold PBS containing 0.1% BSA and 5 mM EDTA. Single-cell suspensions were stained with the following fluorochrome conjugates: CD5 (PE Cy5, PE, or APC), CD19 (PE Cy5.5, Pacific Blue, or APC), CD11b (Pacific blue or PE), F4/80 (APC), CD21 (APC), CD23 (PE), Gr-1 (PE Cy7), B220 (APC-Cy7), CD80/86 (biotin-Qdot605-streptavidin), CD4 (FITC), CD3 (PerCP-Cy5.5), and IgM (Alexa Fluor 700). Sorting of cells used a FACS-Aria or a Fortessa (BD) equipped with four lasers and optics for 22-parameter analysis. Analysis was done using FlowJo.

TLR Binding Assays. Commercially available HEK293 cells transfected with murine TLR4, MD-2, CD14, or TLR2 and an inducible secreted embryonic alkaline phosphatase (InVivoGen) were plated in a 96-well plate. The secreted embryonic alkaline phosphatase (SEAP) reporter gene in the cells is under the control of an IL-12 p40 minimal promoter fused to five NF- κ B and AP-1 binding sites. Stimulation with either a TLR4 or TLR2 ligand activates NF- κ B and AP-1,

which induces the production of SEAP. Levels of the secreted alkaline phosphatase measured in the cell culture medium are proportional to the stimulation of the TLR pathway. Background levels are measured using HEK-Blue Null cells, which are transfected with the alkaline phosphatase but not the TLR receptor. The TLR4-transfected cells were grown to confluence and 2, 1, 0.2 μ g of LPS, or 10 μ g of a set of amyloidogenic peptides were added to each well in duplicate in HEK-Blue detection medium (InVivoGen). In the case of the TLR2 transfected cells, PAM2CSK4 was the positive control, and only 2 μ g of LPS were assayed. The plates were incubated for 12 h at 37 °C, and the resulting blue color measured by reading the absorption at 650 nm.

ACKNOWLEDGMENTS. We thank Xuhuai Ji (microarray), Bianca Gomez (flow cytometry), Kitty Lee (microscopy), Megan Phillips, and Jeffrey Waters for their technical assistance. The microarray was performed in the Stanford Human Immune Monitoring Core. Cell sorting/flow cytometry analysis for this project was done on an instrument in the Stanford Shared FACS Facility obtained using National Institutes of Health S10 Shared Instrument Grant S10RR025518-01. The microscopy was performed on a shared confocal microscope supported, in part, by Award Number 1S10OD010580 from the National Center for Research Resources. This work was funded by a fellowship from Novo Nordisk (to M.P.K.); National Institutes of Health Grant 1R43AI108014-01A1 (to J.B.R.); and the National Multiple Sclerosis Society (L.S.).

- Kurnellas MP, Adams CM, Sobel RA, Steinman L, Rothbard JB (2013) Amyloid fibrils composed of hexameric peptides attenuate neuroinflammation. *Sci Transl Med* 5(179):179ra42.
- Kurnellas MP, et al. (2014) Mechanisms of action of therapeutic amyloidogenic hexapeptides in amelioration of inflammatory brain disease. *J Exp Med* 211(9):1847–1856.
- Axtell RC, Raman C, Steinman L (2013) Type I interferons: Beneficial in Th1 and detrimental in Th17 autoimmunity. *Clin Rev Allergy Immunol* 44(2):114–120.
- Ghosh EE, et al. (2010) Two physically, functionally, and developmentally distinct peritoneal macrophage subsets. *Proc Natl Acad Sci USA* 107(6):2568–2573.
- Montecino-Rodriguez E, Leathers H, Dorshkind K (2006) Identification of a B-1 B cell-specified progenitor. *Nat Immunol* 7(3):293–301.
- Bowman EP, et al. (2000) Developmental switches in chemokine response profiles during B cell differentiation and maturation. *J Exp Med* 191(8):1303–1318.
- Cyster JG, et al. (1999) Chemokines and B-cell homing to follicles. *Curr Top Microbiol Immunol* 246:87–92, discussion 93.
- Howard M, O'Garra A (1992) Biological properties of interleukin 10. *Immunol Today* 13(6):198–200.
- O'Garra A, et al. (1992) Ly-1 B (B-1) cells are the main source of B cell-derived interleukin 10. *Eur J Immunol* 22(3):711–717.
- O'Garra A, Howard M (1992) IL-10 production by CD5 B cells. *Ann N Y Acad Sci* 651:182–199.
- Wolf SD, Dittel BN, Hardardottir F, Janeway CA, Jr (1996) Experimental autoimmune encephalomyelitis induction in genetically B cell-deficient mice. *J Exp Med* 184(6):2271–2278.
- Lampropoulou V, et al. (2008) TLR-activated B cells suppress T cell-mediated autoimmunity. *J Immunol* 180(7):4763–4773.
- Fillatreau S, Sweeney CH, McGeachy MJ, Gray D, Anderton SM (2002) B cells regulate autoimmunity by provision of IL-10. *Nat Immunol* 3(10):944–950.
- Maseda D, et al. (2013) Peritoneal cavity regulatory B cells (B10 cells) modulate IFN- γ +CD4+ T cell numbers during colitis development in mice. *J Immunol* 191(5):2780–2795.
- Mauri C, Gray D, Mushtaq N, Londei M (2003) Prevention of arthritis by interleukin 10-producing B cells. *J Exp Med* 197(4):489–501.
- Blair PA, et al. (2009) Selective targeting of B cells with agonistic anti-CD40 is an efficacious strategy for the generation of induced regulatory T2-like B cells and for the suppression of lupus in MRL/lpr mice. *J Immunol* 182(6):3492–3502.
- Bodhankar S, Chen Y, Vandenbark AA, Murphy SJ, Offner H (2013) IL-10-producing B-cells limit CNS inflammation and infarct volume in experimental stroke. *Metab Brain Dis* 28(3):375–386.
- Shen L, et al. (2015) B-1a lymphocytes attenuate insulin resistance. *Diabetes* 64(2):593–603.
- Tedder TF, Matsushita T (2010) Regulatory B cells that produce IL-10: A breath of fresh air in allergic airway disease. *J Allergy Clin Immunol* 125(5):1125–1127.
- Margry B, et al. (2014) Activated peritoneal cavity B-1a cells possess regulatory B cell properties. *PLoS One* 9(2):e88869.
- Baumgarth N, Waffarn EE, Nguyen TT (June 9, 2015) Natural and induced B-1 cell immunity to infections raises questions of nature versus nurture. *Ann N Y Acad Sci*, 10.1111/nyas.12804.
- Mauri C, Bosma A (2012) Immune regulatory function of B cells. *Annu Rev Immunol* 30:221–241.
- Yanaba K, Bouaziz JD, Matsushita T, Tsubata T, Tedder TF (2009) The development and function of regulatory B cells expressing IL-10 (B10 cells) requires antigen receptor diversity and TLR signals. *J Immunol* 182(12):7459–7472.
- Yoshizaki A, et al. (2012) Regulatory B cells control T-cell autoimmunity through IL-21-dependent cognate interactions. *Nature* 491(7423):264–268.
- Yang Y, Tung JW, Ghosh EE, Herzenberg LA, Herzenberg LA (2007) Division and differentiation of natural antibody-producing cells in mouse spleen. *Proc Natl Acad Sci USA* 104(11):4542–4546.
- Ather JL, et al. (2011) Serum amyloid A activates the NLRP3 inflammasome and promotes Th17 allergic asthma in mice. *J Immunol* 187(1):64–73.
- Halle A, et al. (2008) The NALP3 inflammasome is involved in the innate immune response to amyloid-beta. *Nat Immunol* 9(8):857–865.
- Masters SL, et al. (2010) Activation of the NLRP3 inflammasome by islet amyloid polypeptide provides a mechanism for enhanced IL-1 β in type 2 diabetes. *Nat Immunol* 11(10):897–904.
- Sheedy FJ, et al. (2013) CD36 coordinates NLRP3 inflammasome activation by facilitating intracellular nucleation of soluble ligands into particulate ligands in sterile inflammation. *Nat Immunol* 14(8):812–820.
- Jay TR, et al. (2015) TREM2 deficiency eliminates TREM2+ inflammatory macrophages and ameliorates pathology in Alzheimer's disease mouse models. *J Exp Med* 212(3):287–295.
- Kitamura D, Roes J, Kühn R, Rajewsky K (1991) A B cell-deficient mouse by targeted disruption of the membrane exon of the immunoglobulin mu chain gene. *Nature* 350(6317):423–426.
- Evans JG, et al. (2007) Novel suppressive function of transitional 2 B cells in experimental arthritis. *J Immunol* 178(12):7868–7878.
- Bouabe H (2012) Cytokine reporter mice: The special case of IL-10. *Scand J Immunol* 75(6):553–567.
- Balabanian K, et al. (2003) Role of the chemokine stromal cell-derived factor 1 in autoantibody production and nephritis in murine lupus. *J Immunol* 170(6):3392–3400.
- Ghosh EE, Sadate-Ngatchou P, Yang Y, Herzenberg LA, Herzenberg LA (2011) Distinct progenitors for B-1 and B-2 cells are present in adult mouse spleen. *Proc Natl Acad Sci USA* 108(7):2879–2884.
- Kawai T, Akira S (2010) The role of pattern-recognition receptors in innate immunity: Update on Toll-like receptors. *Nat Immunol* 11(5):373–384.
- Rossol M, et al. (2011) LPS-induced cytokine production in human monocytes and macrophages. *Crit Rev Immunol* 31(5):379–446.
- Bode JG, Ehrling C, Häussinger D (2012) The macrophage response towards LPS and its control through the p38(MAPK)-STAT3 axis. *Cell Signal* 24(6):1185–1194.
- DuBoff B, Feany M, Götz J (2013) Why size matters—Balancing mitochondrial dynamics in Alzheimer's disease. *Trends Neurosci* 36(6):325–335.
- Yenson V, Baumgarth N (2014) Purification and immune phenotyping of B-1 cells from body cavities of mice. *Methods Mol Biol* 1190:17–34.
- Moore KW, O'Garra A, de Waal Malefyt R, Vieira P, Mosmann TR (1993) Interleukin-10. *Annu Rev Immunol* 11:165–190.
- Yanaba K, et al. (2008) B-lymphocyte contributions to human autoimmune disease. *Immunol Rev* 223:284–299.
- Sriram S, Solomon D, Rouse RV, Steinman L (1982) Identification of T cell subsets and B lymphocytes in mouse brain experimental allergic encephalitis lesions. *J Immunol* 129(4):1649–1651.
- Bouaziz JD, Yanaba K, Tedder TF (2008) Regulatory B cells as inhibitors of immune responses and inflammation. *Immunol Rev* 224:201–214.
- Wender PA, et al. (2000) The design, synthesis, and evaluation of molecules that enable or enhance cellular uptake: Peptoid molecular transporters. *Proc Natl Acad Sci USA* 97(24):13003–13008.